

Detonation Onset in Shock Wave Reflected from a Wedge

Smirnov N.N.^{*1,2}, Penyazkov O.G.³, Sevrouk K.L.³, Nikitin V.F.¹, Stamov L.I.^{1,2}, Tyurenkova V.V.^{1,2}

(1) – Moscow Lomonosov State University, Moscow 119992, Russia

(2) – Scientific Research Institute for System Analysis of Russian Academy of Sciences, Moscow 117218, Russia

(3) – Lykov's Heat and Mass Transfer Institute of National Academy of Science of Belarus, Minsk, P.Brovki 15, Belarus

1 Abstract

The paper presents results of numerical and experimental investigation of mixture ignition and detonation onset in shock wave reflected from inside a wedge. Contrary to existing opinion of shock wave focusing being the mechanism for detonation onset in reflection from a wedge or cone, it was demonstrated that along with the main scenario there exists a transient one, under which focusing causes ignition and successive flame acceleration bringing to detonation onset far behind the reflected shock wave. Several different flow scenarios manifest in reflection of shock waves all being dependent on incident shock wave intensity: reflecting of shock wave with lagging behind combustion zone, formation of detonation wave in reflection and focusing, and intermediate transient regimes.

2 Introduction

Control of detonation onset is necessary in perspective pulse detonation engines using hydrogen-air mixtures in the working cycle, which are under development now. In our experimental and numerical studies we'll use hydrogen fuel because, on one hand, it is a very perspective fuel making the engine exhaust much cleaner than that for hydrocarbon combustion [1,2], and on the other hand, chemical kinetics for hydrogen – air mixtures combustion are well developed [3-8]. Numerical simulations of pulse detonation engines operation aimed at increasing their efficiency and developing control strategies consume much time and computational recourses. The thermodynamic efficiency of Chapman – Jouguet detonation as compared with slow combustion modes is due to the minimal entropy of the exhaust jet [9].

3 Mathematical model.

In order to calculate multi-component gas dynamics with chemical reactions including transport phenomena effects and turbulence we use the following set of simultaneous equations:

$$\frac{\partial \rho_k}{\partial t} + \frac{\partial}{\partial x_j} (\rho_k u_j - J_{kj}) = \dot{\omega}_k, \quad \frac{\partial \rho u_i}{\partial t} + \frac{\partial}{\partial x_j} (\rho u_i u_j) + \frac{\partial p}{\partial x_i} = \frac{\partial \tau_{ij}}{\partial x_j}, \quad \frac{\partial E}{\partial t} + \frac{\partial}{\partial x_j} ((E + p)u_j - J_{Q,j}) = \frac{\partial u_i \tau_{ij}}{\partial x_j}.$$

In equations, index k takes values $1 \dots N_C$ (number of components), and indices i, j – values $1, 2, 3$

* Corresponding author: e-mail: ebifsun1@mech.math.msu.su

(number of dimensions); repeated indices presume summation. In total, there are $N_C + 4$ differential equations in the set. The stresses tensor, besides the pressure part, the diffusion flux, and the thermal flux are determined accounting for molecular and turbulent transfer coefficients. There is summation upon the repeating indices in equations. Differential equations are to be complemented with algebraic relations and algebraic representations for chemical and mass and energy sources. We use the two-equation model of Wilcox k-omega turbulence model [10]. Boundary conditions on the walls in our model correspond to the impermeability condition. For viscous turbulent flow additional boundary condition is used, which determines the shear stress on the wall τ_w based on the data of k, ω turbulence model. Details of detonation onset simulation peculiarities can be found in [9, 11]. Two different shock-capturing methods were tested in numerical simulations:

1) Explicit second-order in space and time method based on the MUSCL-interpolation of variables on a face at a convective flux calculation. Interpolation direction choice and pressure interpolation were performed by means of AUSMP method. Parallel execution support was implemented using OpenMP library.

2) Explicit third-order in space and second-order in time scheme based on the Kurganov – Levy method [12]. The method was implemented on a regular grid (rectangular parallelepipeds). The source codes were written in FORTRAN. The equations of state have the following form:

$$\rho = \sum_{k=1}^{N_C} \rho_k, \quad p = R_G T \sum_{k=1}^{N_C} \frac{\rho_k}{W_k}, \quad h = R_G T \sum_{k=1}^{N_C} \left(\frac{\rho_k}{\rho} \frac{\hat{H}_k(T)}{W_k} \right), \quad E = \rho \left(h - \frac{p}{\rho} \right) + \rho \frac{u^2}{2} + \rho K$$

The following components were used: $\{H_2O, OH, H, O, HO_2, H_2O_2, O_2, H_2, N_2\}$. In calculations we used kinetic mechanism of hydrogen combustion without nitrogen oxides formation (those reactions are reasonably slow to influence detonation and combustion and usually are calculated a posteriori). As a basis we took Maas-Warnatz mechanism [8], which was then modified for high pressures [11].

4 Initial conditions and computation domain.

The problem simulating processes in the final section of the cylindrical shock tube was regarded. The geometry and size of computational domain coincides with that in the shock tube used in experiments. The shock tube diameter was $2R=76$ mm, length – $L=720$ mm. (Fig. 1).

The tube is filled in with stoichiometric hydrogen-air mixture with $[H_2]:[O_2]:[N_2]=2:1:3.76$. A special end section, described by (2.2), was installed into the tube providing a wedge cavity with the opening angle 90° . A plane shock wave with velocity D is falling and reflecting from the wedge, and processes accompanying focusing are regarded.

Initial state of the gaseous mixture before plane shock wave near the right hand end of the tube is given by $P_0, T_0, \mathbf{u}_{ini} = \mathbf{0}$. The state of gas behind the shock wave was described by the following parameters: P_1, T_1 and $\mathbf{u}_1 = \{U_1, 0, 0\}$. At $t = 0$ the position of shock wave is $x = x_0 = 0.67$ m. The initial conditions variation corresponds to that in experiments. The initial data for all cases regarded is provided in the Table 1.

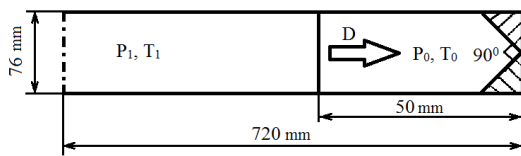


Figure1. Computational domain.

Table 1	WEDGE02R	WEDGE19Q	WEDGE08P
T_0, K	294	293	295
P_0, bar	0.28	0.37	0.12
T_1, K	593	421	559
P_1, bar	1.85	1.13	0.66
$U_1, m/s$	672	362	617
$D, m/s$	969	675	915

5 Simulation results.

Fig. 2 illustrates distribution of axial velocity for successive time moments in cross-section planes: meridional and orthogonal, for numerical experiments WEDGE02R. The section $x \in [0.52, 0.72]$ m is shown.

In Fig. 2, velocity component in the Ox direction is shown in Oxy and Oxz meridional planes. Negative velocity values correspond to motion from right to the left. It is seen from Fig. 2.2 that the time moment 0.06 ms is characterized by a sharp increase of flow velocity in the tip of the cone.

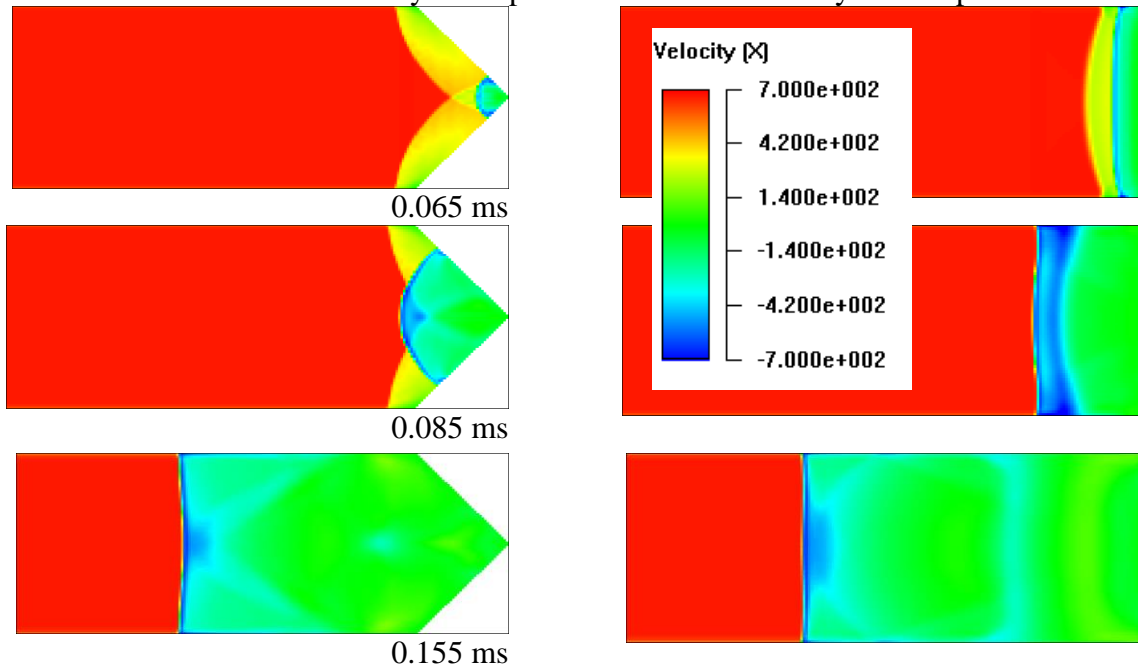


Figure 2. Axial velocity fields in (m/s) on focusing shock wave and detonation onset in reflection from a wedge surface. Meridian cross-sections Oxy (left) and Oxz (right); version WEDGE02R.

At time 0.065 ms onset of detonation is observed in the tip of the wedge. Then detonation wave propagates outside the wedge.

Fig. 3 illustrates successive stages of the process of deflagration to detonation transition after reflecting of shock wave from a wedge for the case WEDGE08P (main parameters are shown in table 2). The initial turbulence level was given by parameters: $K_o = 3000$ J/kg, $R_{T,o} = v_{T,o} / v_o = 35$. The working zone of computational domain shown in figures: $x \in [0.42, 0.72]$ m.

In Fig. 3 axial velocity fields in (m/s) on focusing shock wave and deflagration to detonation transition in reflection from a wedge surface in meridian cross-sections Oxy (left) and Oxz (right) for successive characteristic times are presented. Velocity field in the Fig. 3 testifies that on reflection of shock wave from the wedge surface cumulative effect is not string enough for the onset of detonation wave. shock wave is reflected. Ignition of mixture in the tip takes place later, and accelerated flame moving in pre-compressed and non-uniformly heated gas in the long run gives birth to local explosion and formation of detonation and retonation waves. Velocity field makes it possible distinguishing between detonation and retonation waves due to positive and negative velocities being depicted in different colours.

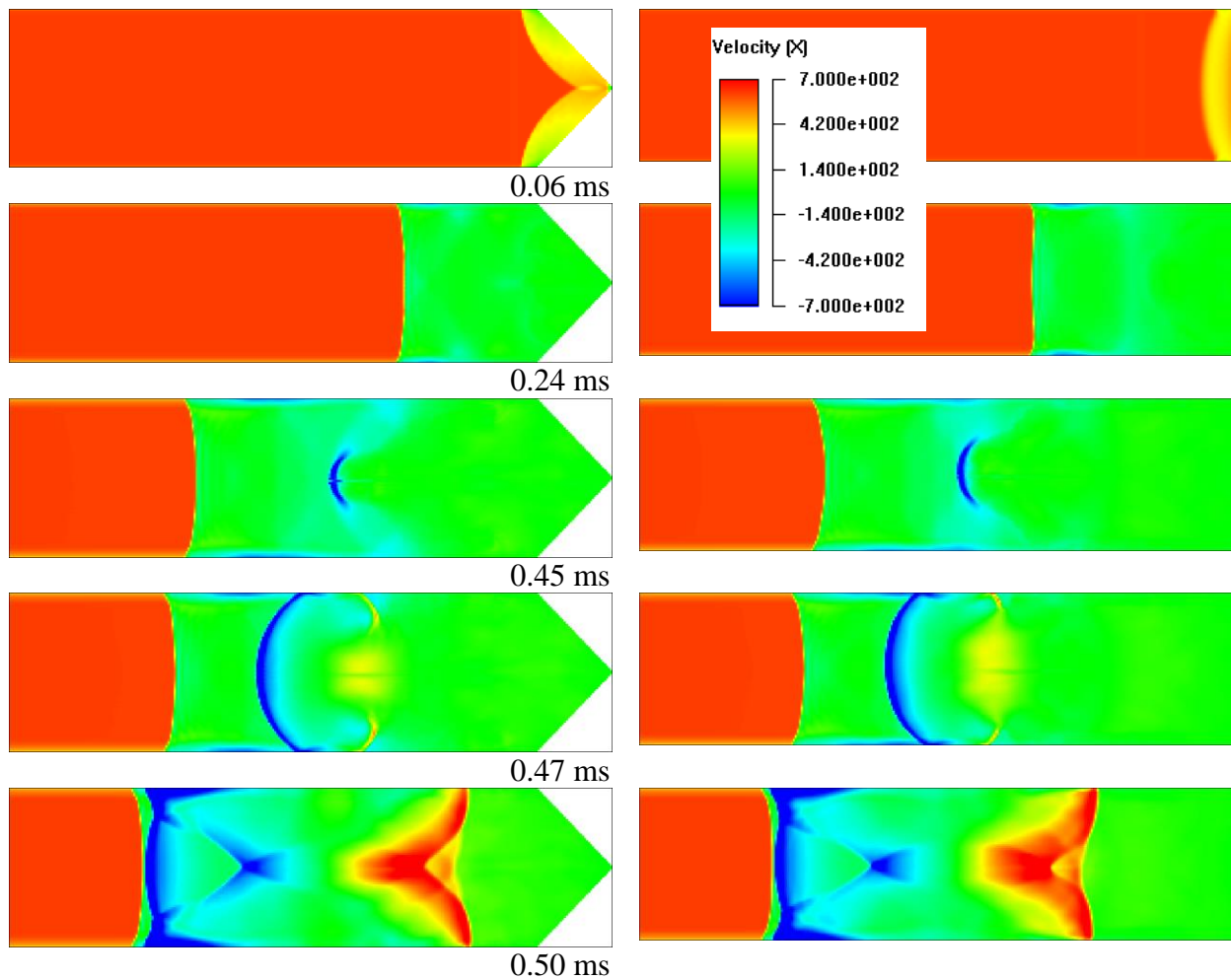


Figure 3. Axial velocity fields in (m/s) on focusing shock wave and deflagration to detonation transition in reflection from a wedge surface. Meridian cross-sections Oxy (left) and Oxz (right); version WEDGE08P.

6 Experimental investigations.

Experimental studies were performed in a shock tube with a wedge cavity in the end. The reflection of shock waves of different intensity were analyzed. Pressure-time history and OH radical emission was recorded. Fig. 4 presents the scheme of measuring section of the shock tube, in which experiments on shock waves focusing were conducted. Similar geometry was used in numerical simulations. In numerical simulations gas dynamic parameters variation in the places of pressure transducers location were recorded as well. The details on experiments can be found in [11].

7 Comparing numerical and experimental results.

Comparison of numerical simulation results and experimental data is performed based on pressure records in five different places after the incident shock reflection.

As it is seen from the figures, onset of detonation due to focusing of a strong shock wave takes place via an overdriven detonation mode. Then detonation wave slows down to a self-sustaining mode. Experimentally measured velocity, as well as calculated using scheme 1, well coincide, but both diverge from Chapman – Jouguet velocity as a limit for the self-sustaining regime. On the other hand, numerical results based on scheme 2 have Chapman – Jouguet velocity as a limit. These differences can

be explained by the effect of turbulence. In reflecting from closed edge the detonation wave propagates through the disturbed and turbulized mixture, which possesses additional turbulent kinetic energy delivered to the mixture by the incident shock wave. Due to this reason, relative detonation wave velocity turns out to be higher than the Chapman – Jouguet velocity calculated disregarding initial mixture turbulization. Numerical model 2 does not take into account turbulent energy production in the flow. Thus it provides the limiting velocity equal to the Chapman – Jouguet value.

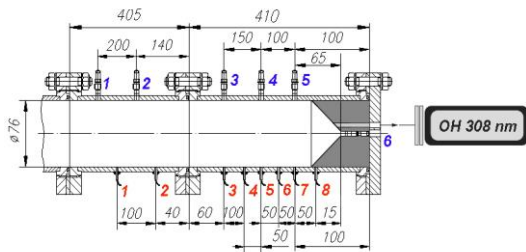


Figure 4. The scheme of the end section of shock tube, wherein measurements were performed for shock waves focusing and reflection experiments. On top and in the center six pressure transducers are located. Opposite 8 ionization probes are located along the bottom wall, and OH detector is located on the back wall close to the axis.

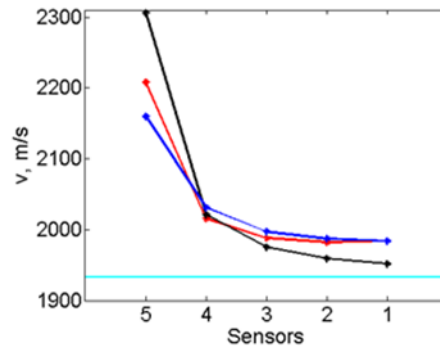


Figure 5. Experimental results on reflected shock wave mean velocity and its comparison with numerical simulations using codes based on scheme 1 and scheme 2, as well as its comparison with equilibrium calculations of Chapman – Jouguet detonation velocity: red curves numbered 3 – experiment, blue curves numbered 1 – numerical solution scheme 1, black curves numbered 2 – numerical solutions scheme 2, marine horizontal line – Chapman – Jouguet velocity. Version WEDGE02R.

Comparison of results of numerical and physical experiments for different initial incident shock wave intensities showed that for relatively weak shock waves, when ignition behind reflected shock does not occur, the difference of numerical and experimental data does not exceed 2.6%, while for incident shock waves of higher intensity, which bring to ignition after reflection and focusing, velocity difference is around 3.5%.

Results presented in Fig. 6 illustrate the intermediate case: after reflection attenuation of a strong shock wave takes place. Then behind the shock wave “explosion in the explosion” occurs, which brings to onset of detonation and retonation waves. Detonation onset takes place via an overdriven mode. (Fig. 7).

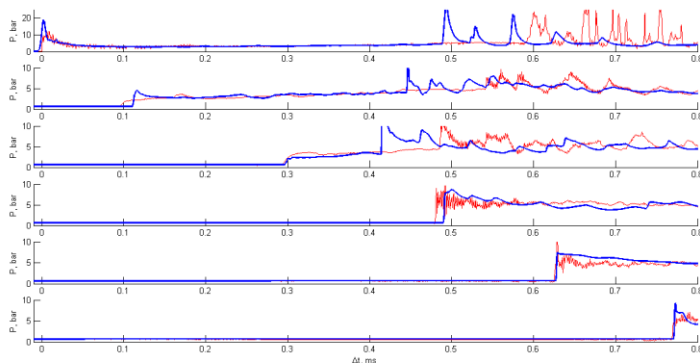


Figure 6. Pressure-time history (bar-ms) in control points after reflection and focusing of shock wave in combustible hydrogen-air mixture: red curves numbered 3 – experiment, blue curves numbered 1 – numerical solution scheme 1, version WEDGE08P.

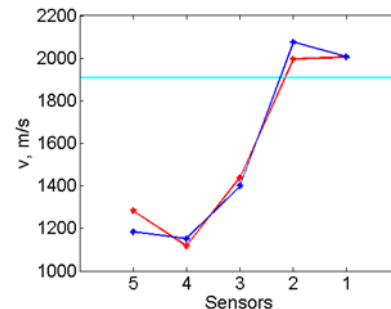


Figure 7. Reflected wave velocity in control points after reflection and focusing of shock wave in combustible hydrogen-air mixture: red curves numbered 3 – experiment, blue curves numbered 1 – numerical solution scheme 1, marine horizontal curve – Chapman-Jouguet velocity, version WEDGE08P

8 Conclusions

Theoretical and experimental studies of detonation initiation due to focusing of a shock wave reflected inside a wedge showed several different flow scenarios in reflection of shock waves all being dependent on incident shock wave intensity: reflecting of shock wave with lagging behind combustion zone, formation of detonation wave in reflection and focusing, and intermediate transient regimes with successive deflagration to detonation transition.

It was demonstrated that onset of detonation due to focusing of a strong shock wave takes place via an overdriven detonation mode. Then detonation wave slows down to a self-sustaining mode.

The transient regime has the following characteristic stages. First, at the tip of the wedge in the center a hot spot appears, which later increases rapidly in all directions, nevertheless lagging behind the reflected shock wave. Combustion wave is thus formed. Second, the combustion zone grows the leading front being unstable. Wrinkles are formed on the leading front, which is noticeable especially in the plane orthogonal to wedge. Third, velocity of combustion wave drastically increases, especially in the wrinkled zone, the wrinkles become deeper. Forth, the zone grows near the axis, which testifies formation “explosion in the explosion” and onset of detonation wave. The detonation wave begins reflecting from side walls of the cylinder and further propagate as detonation and retonation waves in all directions.

Comparison of results made it possible to validate the developed 3-d transient mathematical model of chemically reacting gas mixture flows incorporating hydrogen – air mixtures. The results of theoretical and numerical experiments made it possible improving kinetic scheme for hydrogen-air mixtures at high pressures.

References

- [1] CHEMKIN. A software package for the analysis of gas-phase chemical and plasma kinetics. CHE-036-1. Chemkin collection release 3.6. Reaction Design, September 2000.
- [2] N.M. Marinov, W.J. Pitz, C.K. Westbrook, M. Hori, N. Matsunaga, An Experimental and Kinetic Calculation of the Promotion Effect of Hydrocarbons on the NO-NO₂ Conversion in a Flow Reactor. Proceedings of the Combustion Institute, Volume 27, pp. 389-396, 1998. (UCRL-JC-129372). UCRL-WEB-204236.
- [3] R.J. Kee, J.A. Miller, and T.H. Jefferson. Chemkin: a general-purpose, problem-independent, transportable Fortran chemical kinetics code package. Sandia National Laboratories Report SAND80-8003 (1980).
- [4]. S. Browne, J. Ziegler, and J. E. Shepherd. Numerical Solution Methods for Shock and Detonation Jump Conditions. GALCIT Report FM2006.006 July 2004-Revised August 29, 2008.
- [5] S. Gordon, and B.J. McBride. Computer Program for Calculation of Complex Chemical Equilibrium Compositions and Applications I. Analysis. NASA RP-1311, October 1994.
- [8] U. Maas, J. Warnatz. Ignition process in hydrogen-oxygen mixtures. Combustion and Flame, 74, No. 1, 1988, pp. 53-69.
- [9] N.N. Smirnov, V.B. Betelin, V.F. Nikitin, Yu.G. Phylippov, Jaye Koo. Detonation engine fed by acetylene-oxygen mixture, Acta Astronautica (2014), vol. 104, 134-146.
<http://dx.doi.org/10.1016/j.actaastro.2014.07.019>
- [10] D.C. Wilcox. Turbulence modeling for CFD. DCW Industries, Inc. 1994.
- [11] Smirnov N.N., Penyazkov O.G., Sevrouk K.L., Nikitin V.F., Stamov L.I., Tyurenkova V.V. Detonation onset following shock wave focusing. Acta Astronautica, 2017. Volume 135, Pages 114-130.
- [12] Kurganov A., Levy D. A third-order semidiscrete central scheme for conservation laws and convection-diffusion equations // SIAM J. SCI. COMPUT. 2001. 22(4). P. 1461–1488.